
Article:
Barker, J and Bauer, GEW (2019) Semiquantum thermodynamics of complex ferrimagnets. Physical Review B, 100 (14). 140401(R). ISSN: 2469-9950

https://doi.org/10.1103/PhysRevB.100.140401

Semi-quantum thermodynamics of complex ferrimagnets

Joseph Barker[1] and Gerrit E.W. Bauer[2,3]

[1]*Institute for Materials Research, Tohoku University, Sendai 980-8577, Japan*
[2]*Institute for Materials Research & AIMR & CSRN, Tohoku University, Sendai 980-8577, Japan*
[3]*Zernike Institute for Advanced Materials, University of Groningen, 9747 AG Groningen, The Netherlands*

High-quality magnets such as yttrium iron garnet (YIG) are electrically insulating and very complex. By implementing a quantum thermostat into atomistic spin dynamics we compute YIG's key thermodynamic properties, viz. the magnon power spectrum and specific heat, for a large temperature range. The results differ (sometimes spectacularly) from simple models and classical statistics, but agree with available experimental data.

Introduction The spin dynamics of electrically insulating magnets often has high quality because the dissipation channel by conduction electron scattering is absent. With few exceptions, they are complex ferrimagnets. Yttrium iron garnet (YIG) with 80 atoms in the unit cell rules with a record low Gilbert damping of long wavelength spin wave excitations or magnons, even at room temperature [1, 2]. The implied exceptionally low disorder and weak coupling with phonons remains a mystery, however. Recently, magnon heat and spin transport were measured in YIG thin films in a non-local spin injection and detection configuration with Pt contacts by means of the spin Hall effect [3] and modelled by spin diffusion [4]. Key parameters of this model are linked to the thermodynamics of the magnetic order, such as the magnon heat capacity, which is difficult to measure because it is orders of magnitude smaller than the phonon heat capacity—at 10 K the magnon and phonon heat capacities are $C_m \approx 0.009$ J kg^{-1} K^{-1} and $C_p \approx 0.270$ J kg^{-1} K^{-1} [5]. They can be separated by magnetic freeze-out of the magnon contribution at temperatures up to a few Kelvin [5, 6]. The magnon heat capacity at higher temperatures has been estimated by extrapolating models that agree with experimental low-temperature results [4, 7]. YIG is often treated as a single-mode ferromagnet with quadratic $\omega \propto \mathcal{D}k^2$ (or isotropic cosine function) dispersion, thereby ignoring higher frequency acoustic and optical modes and temperature dependence of the exchange stiffness $\mathcal{D}$. Furthermore, magnon-magnon interactions are also commonly neglected or treated in a mean field approximation. Statistical approaches also have issues, such as the use of classical (Johnson-Nyquist) thermal noise at low temperatures [8].

In this Letter we introduce a numerical method that avoids all of these shortcomings. It allows us to carry out material-dependent thermodynamic calculations that are quantitatively accurate with a small number of parameters that can be determined independently. The crucial ingredient is a thermostat for Planck quantum (rather than Rayleigh–Jeans classical) statistics in an atomistic spin dynamics framework [9].

With the inclusion of quantum thermal statistics we find quantitative agreement for YIG with available experiments at low temperatures. The computed spin wave dispersion as a function of temperature agree well with results from neutron scattering. This low temperature quantitative benchmarking imbues trust in the technique for calculating thermodynamic functions and allows access to quantities such as the magnon heat capacity at room temperature that turns out to be an order of magnitude larger than previous estimates.

Method We address the thermodynamics by computing the atomistic spin dynamics in the long (ergodic) time limit to generate canonical ensembles of spins. The magnetic moments ('spins') in this model are treated as classical unit vectors $\mathbf{S}$, an excellent approximation for the half-filled 3d-shell of the iron cations in YIG with $\mathcal{S} = 5/2$ and magnetic moment $\mu_s = g\mu_B\mathcal{S}$, where $g \approx 2$ is the electron g-factor and μ_B the Bohr magneton.

The Heisenberg Hamiltonian $\mathscr{H} = -\frac{1}{2}\sum_{ij} J_{ij}\mathbf{S}_i \cdot \mathbf{S}_j$ contains the (super)-exchange parameters J_{ij} between spins on sites i and j, which are determined by fits to inelastic neutron scattering data [10]. Recently, the magnon dispersions were measured again with higher resolution [11], allowing an improved parameterization of the six nearest-neighbors exchange constants, which we adopt in the following. We add a Zeeman term $\mathscr{H} = -\sum_i \mu_{s,i}\mathbf{H}_{\text{ext}} \cdot \mathbf{S}_i$ with $\mathbf{H}_{\text{ext}} = H_z = 0.1$ T, to fix the quantization axis. On each lattice site 'i' the spin dynamics obey the Landau-Lifshitz equation of motion [12]:

$$\frac{\partial \mathbf{S}_i}{\partial t} = -|\gamma|\left(\mathbf{S}_i \times \mathbf{H}_i + \eta \mathbf{S}_i \times (\mathbf{S}_i \times \mathbf{H}_i)\right), \qquad (1)$$

where $\gamma = g\mu_B/\hbar$ is the gyromagnetic ratio and η is a damping constant. Each spin feels an effective magnetic field $\mathbf{H}_i = \boldsymbol{\xi}_i - (1/\mu_{s,i})\partial\mathscr{H}/\partial\mathbf{S}_i$, where $\boldsymbol{\xi}_i$ are stochastic processes controlled by the thermostat at temperature T. $\langle\xi_{i\alpha}\rangle = 0$ and the correlation function in frequency space is governed by the fluctuation-dissipation theorem (FDT) $\langle\xi_{i\alpha}\xi_{j\beta}\rangle_\omega = 2\eta\delta_{ij}\delta_{\alpha\beta}\varphi(\omega,T)/\mu_{s,i}$, where the Kronecker δ's reflect the assumption that the fluctuations between lattice sites i, j and Cartesian coordinates α, β are uncorrelated. $\varphi(\omega,T)$ describes the temperature dependence of the noise power and is chosen such that the steady-state distribution functions obey equilibrium thermal statistics. By not approximating the spin Hamiltonian by a truncated Holstein-Primakoff expansion, our approach includes magnon-magnon interactions to all orders [13].

Atomistic spin dynamics methods generally assume the classical limit of the FDT with frequency independent (white) noise $\varphi(\omega,T) = k_BT$, i.e. *all* magnons are stimulated.

The energy equipartition of the coupled system results in the Rayleigh-Jeans magnon distribution. However, this is only valid when the thermal energy is much larger than that of the magnon mode k under consideration, i.e. when $k_BT \gg \hbar\omega_k$, while the energies of the YIG magnon spectrum–and that of most room temperature magnets–extend up to $\hbar\omega_{\mathbf{k}}/k_B \approx 1000$ K [1]. A classical thermostat therefore generates too many high energy magnons, which, for example, overestimates the broadening by magnon scattering and leads to other predictions that can be very wrong.

According to the quantum FDT for magnons [14, 16]

$$\varphi(\omega, T) = \frac{\hbar\omega}{\exp\left(\hbar\omega/k_BT\right) - 1}, \tag{2}$$

which means that equipartition is replaced by Planck statistics of the magnons at temperature T. Quantum statistics in classical spin systems can partially be mimicked through a post-process rescaling of the temperature [15] or by using temperature-dependent frequencies that rely on analytic expressions for the low temperature spectrum [16]. These approaches cannot be used to evaluate all thermodynamic properties and are not suitable to treat complex magnets such as YIG. We therefore adopt here the 'quantum thermostat' introduced earlier in molecular dynamics [17, 18], i.e., a correlated noise source that obeys the quantum FDT. This is "colored"noise, but very different from the one used to describe classical memory effects in the heat bath [19, 20].

We implement the quantum statistics by generating correlated fluctuating fields $\boldsymbol{\xi}_i(t)$ numerically in time that obey the FDT in the frequency domain. Savin et al. [18] employ a set of stochastic differential equations that produce the required distribution function. We adjust this method to spin dynamics problems, referring the reader to Ref. [18] and the supplementary information S1 for the technical details [21]. The solution is a dimensionless stochastic process $\Phi_{i\alpha}(t)$ with the spectrum of Eq. (2). The dimensionful noise in the spin dynamics reads

$$\xi_{i\alpha}(t) = k_BT\sqrt{\frac{2\eta\mu_{s,i}}{\gamma\hbar}}\Phi_{i\alpha}(t). \tag{3}$$

When we agitate the model of classical spins with these stochastic fields, the excitations of the ground state (magnons) obey quantum statistics, quite analogous to quantized phonons in a classical ball-spring lattice. This approach may loosely be called 'semi-quantum' and works very well for the large Fe^{3+} spin in YIG with $\mathcal{S} = 5/2$ ($\mu_s = 5\mu_B$), but requires more scrutiny for spin $\mathcal{S} = 1/2$ (see Supplement S2 [21]).

We integrate equation (1) using the Heun method with time step $\Delta t = 0.1$ fs. The stochastic differential equations of the thermostat are integrated using the fourth-order Runge-Kutta method with the same time step. The exchange parameters from Ref. [11]—scaled by $\mathcal{S}^2$ for to unit spins—read $J_1 = -42.5$, $J_2 = -3.25$, $J_{3a} = 0$, $J_{3b} = -6.875$, $J_4 = 0.4375$, $J_5 = -2.9375$, $J_6 = 0.5625$ meV for successive nearest neighbours. For the magnon spectrum we use $\eta = 2 \times 10^{-4}$ representing the low Gilbert damping of YIG. For thermodynamic calculations we use over-damped dynamics with $\eta = 0.1$ for faster convergence. Thermodynamic quantities (energy, magnetization) were calculated for 5 ns, discarding the initial equilibration period (generally below 0.1 ns). The remaining time series are used to calculate the thermodynamic averages. 5 independent stochastic trajectories were calculated and averaged for each data point. Error bars defined as three times the standard deviation for thermodynamic averages between these trajectories were mostly smaller than the data points in the figures.

Magnon spectrum We compare now the magnon spectrum computed with the quantum thermostat with our previous work with classical statistics (and older exchange constants from Ref. [1]) [9]. Results for low (5 K) and room (300 K) temperature are shown in Fig. 1a. The classical thermostat overestimates the number of high-energy magnons and therefore the broadening of the optical modes at higher temperatures. With quantum statistics, the high-energy optical modes are well resolved at room temperature and should be observable by inelastic neutron scattering with large frequency transfer. The agreement between the calculated and measured [10] temperature dependence of the exchange gap between optical and acoustic modes at the Γ point, shown in Fig. 1 b, is improved, especially in the low temperature regime.

Magnetization The magnetization at low temperatures $m_z = 1 - \frac{1}{\mathcal{S}}\sum_{\mathbf{k}\nu}\langle n_{\mathbf{k}\nu}\rangle_T$, where $\langle n_{\mathbf{k}\nu}\rangle_T$ is the distribution of magnons with wave vector $\mathbf{k}$ and band index ν in the first Brillouin zone, cannot be calculated correctly with classical statistics [22] (at higher temperatures the expression does not hold since magnon-magnon interactions are important). This is obvious already for the single parabolic band, non-interacting magnon gas model for which

$$1 - m_z(T) = v_{\text{ws}}\frac{1}{\mathcal{S}}\frac{\Gamma\left(\frac{3}{2}\right)\zeta\left(\frac{3}{2}\right)}{2\pi^2}\left(\frac{k_BT}{\mathcal{D}}\right)^{3/2} \tag{4}$$

where $\omega_k = \mathcal{D}k^2$, spin-wave stiffness $\mathcal{D} = 2\mathcal{S}\mathcal{J}a^2$, lattice constant a, v_{ws} volume of the Wigner-Seitz cell, while $\Gamma(x)$ and $\zeta(x)$ are the gamma and Riemann zeta functions. The $T^{3/2}$ dependence is known as Bloch's law [23].

In the ferrimagnet YIG the total magnetization is made up by two oppositely aligned sublattices with slightly different temperature dependent magnetizations. At low temperatures they are rigidly locked to an antiparallel configuration by the strong nearest neighbor exchange. At energies $\hbar\omega_{\mathbf{k}}/k_B \lessapprox 30$ K YIG's magnon dispersion is known to be quadratic and its magnetization obeys Bloch's $T^{3/2}$ law [24]. The expected deviations at higher temperatures can be assessed by our method. We calculate the magnetization at temperature T as an average $\langle\cdots\rangle_T$ over the spin configurations at many times over a 1 ns trajectory $\mathbf{m}(T) = \langle N^{-1}\sum_i^N \mu_{s,i}\mathbf{S}_i\rangle_T / \langle N^{-1}\sum_i^N \mu_{s,i}\mathbf{S}_i\rangle_{T=0}$, where $N = 655,360$ is the total number of spins in the simulation.

Fig. 2 exposes the obvious problem of classical statistics

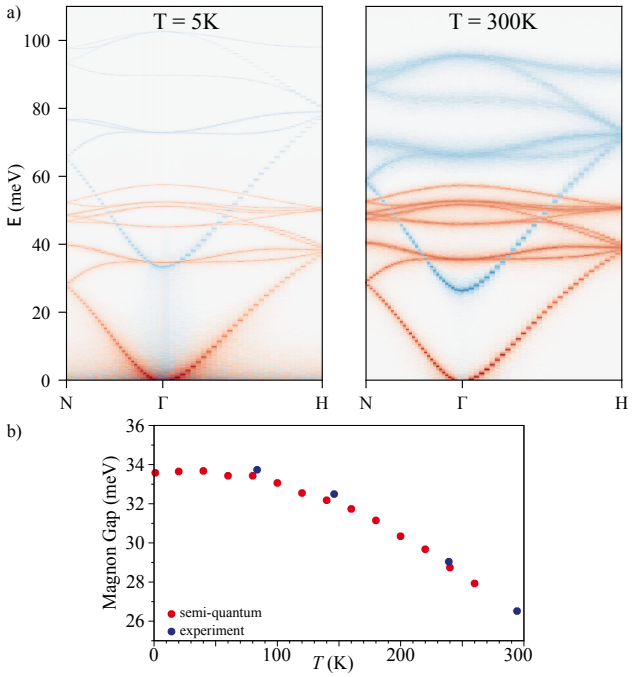

FIG. 1. a) YIG magnon spectrum at $T = 5$ K and $T = 300$ K calculated using the quantum thermostat and the exchange parameters of Ref. 11. The color intensity is adjusted on a log scale such that all modes are visible (even for extremely low occupation) and is different for both figures. The red/blue color shows the +/- polarization of the magnons. b) Magnon gap between optical and acoustic modes at Γ. Experimental data are adopted from neutron scattering experiments [10].

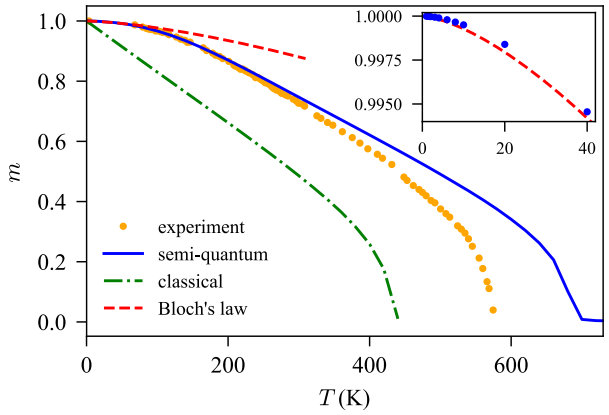

FIG. 2. Temperature dependent magnetization of YIG calculated using classical and semi-quantum spin dynamics. The experimental points are from [27] and Bloch's law from Eq. (4) with $\mathcal{D} = 85.2 \times 10^{-41}$ Jm^2 [11], which in YIG is temperature independent until close to the Curie temperature. The inset is a close up of the semi-quantum method (blue circles) in the low temperature regime where Bloch's law (dashed red line) is valid.

to compute magnetizations at low temperatures: The magnetization decreases much more rapidly with temperature than Bloch's law (and as observed in experiments). The results with the quantum thermostat, on the other hand, adhere to Bloch's law for $T < 30$ K (see inset) but also agree well with experiments that signal a breakdown of $T^{3/2}$ scaling, at least until ~ 300 K.

The Curie temperatures for the classical ($T_C = 420$ K) and quantum thermostated systems ($T_C = 680$ K) are quite different, while the observed $T_C = 550$ K lies between the theoretical values. In contrast to classical results that obey equipartition, the Curie temperature of quantum approaches depend on S and we find this also in our semi-quantum approach. For a simple ferromagnetic BCC lattice our computed Curie temperatures agree well with those obtained by semi-analytic approaches [25] for a large range of $\mathcal{S}$ (see supplementary Fig. S3). The overestimation of T_C compared to the experiment might be caused by exchange parameters that are slightly too large since the neutron scattering data are fitted only up to 90 meV which does not cover the magnon modes with highest energy. Also, the choice of $\mathcal{S} = 5/2$ ($\mu_s = 5\mu_B$) in extracting the exchange parameters does not fully agree with with measured values of $\mu_{s,a} = 4.11\mu_B$ and $\mu_{s,d} = 5.37\mu_B$ for the octahedral and tetrahedral sites [26]. Hence, a more accurate set of parameters, fitted to neutron scattering data for large energy transfers or calculated from first principles, should solve this discrepancy.

Heat Capacity The magnon heat capacity per unit volume $C_m = V^{-1}(\partial U_m/\partial T)_V$ is the change in the internal magnetic energy U_m with temperature at constant volume V. It can be calculated from the magnon spectrum as $C_m = V^{-1}(\partial/\partial T)\sum_{\mathbf{k}\nu}\hbar\omega_{\mathbf{k}\nu}\langle n_{\mathbf{k}\nu}\rangle$, where $\langle n_{\mathbf{k}\nu}\rangle$ is the Planck distribution. In the low temperature limit magnons occupy only states close to $k = 0$, where the magnon dispersion of ferromagnets is parabolic. For a single parabolic magnon band [13]

$$C_m(T) = \frac{1}{V}\frac{5}{8}\frac{\Gamma\left(\frac{5}{2}\right)\zeta\left(\frac{5}{2}\right)}{\pi^2}k_B\left(\frac{k_BT}{\mathcal{D}}\right)^{3/2}, \qquad (5)$$

where $\Gamma(x)$ and $\zeta(x)$ are the Gamma and Riemann zeta functions.

The proportionality $C_m \propto T^{3/2}$ should hold for YIG up to energies of $\hbar\omega_{\mathbf{k}}/k_B \lessapprox 30$ K. Rezende and López Ortiz [7] calculated the heat capacity for acoustic magnons with finite band-width, but neglected optical magnons that contribute to the heat capacity at elevated temperatures. They found that C_m saturates at 150 K, i.e. when the magnon occupation reaches the upper band edge.

Here we calculate the heat capacity including all magnon modes and their interactions. We calculate C_m from the energy fluctuations in the canonical ensemble $\langle U_m\rangle_T = (1/Z_m)\sum_{\mathbf{k}\nu}\hbar\omega_{\mathbf{k}\nu}\exp(-\hbar\omega_{\mathbf{k}\nu}/k_BT)$, where $Z_m = \sum_{\mathbf{k}\nu}\exp(-\hbar\omega_{\mathbf{k}\nu}/k_BT)$ is the partition function. Then $C_m = \left(\langle U_m^2\rangle_T - \langle U_m\rangle_T^2\right)/(Vk_BT^2)$, where in a simulation $\langle\cdots\rangle_T$ is an average over a large time interval at a constant temperature and V is the volume of the system.

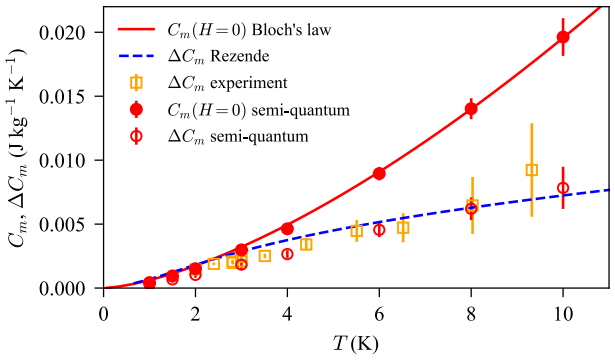

FIG. 3. Low-temperature magnon heat capacity of YIG calculated with quantum statistics (red circles) compared to Bloch's law (red solid line). $\Delta C_m = C_m(H = 0\mathrm{T}) - C_m(H = 7\mathrm{T})$ calculated with quantum statistics (red open circles) is compared with experimental data from Boona and Heremans Ref. 5 (orange open squares) as well as a single magnon band model. [7] (blue dashed line). The error bars on simulated data represent 3 standard deviations across 5 independent stochastic trajectories.

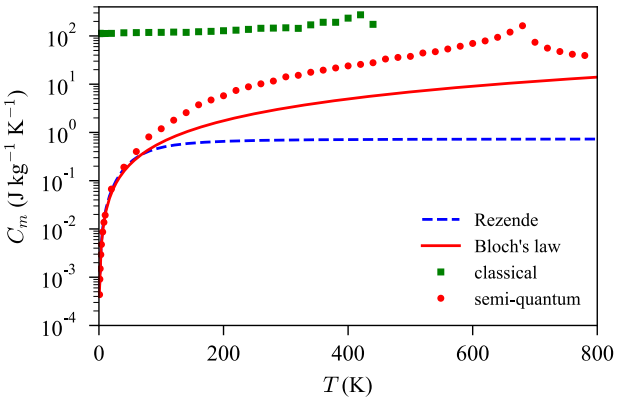

FIG. 4. YIG magnon heat capacity calculated over a larger temperature range with the semi-quantum model (red circles), classical model (green squares), compared with Bloch's law (solid red line) and the single-band model [7] (dashed blue line).

Figure 3 shows the low temperature region where the magnon dispersion is, to a good approximation, parabolic and $C_m \propto T^{3/2}$. Calculations using quantum statistics give an excellent agreement with Bloch's law. The experimental data in Figure 3 have been collected in the range $T = 2 - 9$ K [5], high enough that dipolar field effects can be disregarded. The measurements were made by freezing the magnons in a 7 Tesla field. Even this large field however does not completely remove the magnon contribution to the heat capacity, especially at the higher end of the temperature range [7]. To make a proper comparison we repeat the experimental procedure in our simulation by computing the difference $\Delta C_m = C_m(H = 0\mathrm{T}) - C_m(H = 7\mathrm{T})$. Our calculations agree well with the observations as well as the single magnon-band model.

Figure 4 illustrates a pronounced difference between the classical and semi-quantum models: classical statistics overestimate the heat capacity by 5 orders of magnitude at low temperatures, and do not depend on temperature in contrast to the quantum statistical result which approaches zero like $T^{3/2}$. In spite of this spectacular (and rather obvious) failure, classical statistics have traditionally been used (and still are) in both Monte-Carlo and atomistic spin dynamics.

At $T > 30$ K non-parabolicities begin and $C_m \propto T^p$ with power $p > 3/2$. At room temperatures Fig. 4 reveals differences between the approaches of two orders of magnitude. The finite-width magnon band model [7] (dashed line on figure 4) saturates prematurely with increasing T because optical and higher acoustic modes become significantly occupied when approaching room temperature [9]. The parabolic band model without high-momentum cut-off (Bloch's law) also strongly underestimates C_m because YIG's magnon density of states is strongly enhanced by the flat bands observed in Fig. 1. The semi-quantum calculation is an order of magnitude larger than both of these heavily approximated approaches, benefiting from the complete description of the magnon spectrum as well as magnon-magnon interactions, while the classical statistics strongly overestimates the heat capacity up to the Curie temperature. Since the magnon heat capacity cannot be measured for $T > 10$ K this is the first critical test of the theories.

Conclusions By enforcing Planck statistics for the magnons in the complex ferrimagnet YIG, we obtain excellent agreement with available inelastic neutron scattering and magnon heat capacity experiments. Our results prove that fundamental thermodynamic equilibrium properties can be predicted with confidence when experimental data are not available, but only when quantum statistics and the full spin wave spectrum are taken into account. The method is not limited to YIG or ordered magnets, but can be directly applied to other complex materials with local magnetic moments such as spin glasses or paramagnets. Our results are a necessary first step to compute non-equilibrium properties such as magnon conductivities and spin Seebeck coefficients, which are essential parameters for future applications of magnonic devices.

ACKNOWLEDGEMENTS

This work was supported by JSPS KAKENHI Grant No. 26103006, the Graduate Program in Spintronics (GP-Spin), Tohoku University and DAAD project 'MaHoJeRo'. The authors thank Jiang Xiao, Yaroslav Tserkovnyak, Rembert Duine and Jerome Jackson for valuable discussion.

[1] Vladimir Cherepanov, Igor Kolokolov, and Victor L'vov, "The saga of YIG: spectra, thermodynamics, interaction and relaxation of magnons in a complex magnet," Phys. Rep. **229**, 81 (1993).

[2] Mingzhong Wu and Axel Hoffmann, eds., *Recent Advances in Magnetic Insulators - From Spintronics to Microwave Applications* (Academic Press, 2013).

[3] L. J. Cornelissen, J. Liu, R. A. Duine, J. Ben Youssef, and B. J. Van Wees, "Long-distance transport of magnon spin information in a magnetic insulator at room temperature," Nat. Phys. **11**, 1022–1026 (2015), arXiv:1505.06325.

[4] L. J. Cornelissen, K. J.H. Peters, G. E.W. Bauer, R. A. Duine, and B. J. van Wees, "Magnon spin transport driven by the magnon chemical potential in a magnetic insulator," Phys. Rev. B **94**, 014412 (2016), arXiv:1604.03706.

[5] Stephen R. Boona and Joseph P. Heremans, "Magnon thermal mean free path in yttrium iron garnet," Phys. Rev. B **90**, 064421 (2014).

[6] R. Douglass, "Heat Transport by Spin Waves in Yttrium Iron Garnet," Phys. Rev. **129**, 1132 (1963).

[7] S. M. Rezende and J. C. López Ortiz, "Thermal properties of magnons in yttrium iron garnet at elevated magnetic fields," Phys. Rev. B **91**, 104416 (2015), arXiv:1504.00895.

[8] J. Oitmaa and Thomas Falk, "Ferrimagnetism in the rare-earth iron garnets: A Monte Carlo study," J. Phys. Condens. Matter **21**, 124212 (2009).

[9] Joseph Barker and Gerrit E. W. Bauer, "Thermal spin dynamics of yttrium iron garnet," Phys. Rev. Lett. **117**, 217201 (2016), arXiv:1607.03263.

[10] J S Plant, "Spinwave dispersion curves for yttrium iron garnet," J. Phys. C Solid State Phys. **10**, 4805–4814 (1977).

[11] Andrew J. Princep, Russell A. Ewings, Simon Ward, Sandor Tóth, Carsten Dubs, Dharmalingam Prabhakaran, and Andrew T. Boothroyd, "The full magnon spectrum of yttrium iron garnet," npj Quantum Mater. **2**, 63 (2017).

[12] We prefer the Landau-Lifshitz rather than the Gilbert damping, because latter affects the frequencies (here governed exclusively by the exchange parameters) by a factor $1/(1+\eta^2)$.

[13] Charles Kittel, *Quantum Theory of Solids* (Wiley, New York, 1963).

[14] L D Landau and E M Lifshitz, *Statistical Physics*, 3rd ed. (Elsevier, 1980).

[15] R. F. L. Evans, U. Atxitia, and R. W. Chantrell, "Quantitative simulation of temperature-dependent magnetization dynamics and equilibrium properties of elemental ferromagnets," Phys. Rev. B **91**, 144425 (2015), arXiv:1409.7397.

[16] C H Woo, Haohua Wen, A A Semenov, S L Dudarev, and Pui-wai Ma, "Quantum heat bath for spin-lattice dynamics," Phys. Rev. B **91**, 104306 (2015).

[17] Hichem Dammak, Yann Chalopin, Marine Laroche, Marc Hayoun, and Jean Jacques Greffet, "Quantum Thermal Bath for Molecular Dynamics Simulation," Phys. Rev. Lett. **103**, 190601 (2009).

[18] Alexander V. Savin, Yuriy A. Kosevich, and Andres Cantarero, "Semiquantum molecular dynamics simulation of thermal properties and heat transport in low-dimensional nanostructures," Phys. Rev. B **86**, 064305 (2012), arXiv:arXiv:1112.5919v2.

[19] U. Atxitia, O. Chubykalo-Fesenko, R. W. Chantrell, U. Nowak, and A. Rebei, "Ultrafast spin dynamics: The effect of colored noise," Phys. Rev. Lett. **102**, 057203 (2009), arXiv:0809.4595.

[20] Andreas Rückriegel and Peter Kopietz, "Rayleigh-Jeans Condensation of Pumped Magnons in Thin-Film Ferromagnets," Phys. Rev. Lett. **115**, 157203 (2015), arXiv:1507.01717.

[21] See Supplemental Material at [URL will be inserted by publisher] for technical details of the quantum thermostat and testing in a simple ferromagnetic system.

[22] M.D. Kuz'min, "Shape of Temperature Dependence of Spontaneous Magnetization of Ferromagnets : Quantitative Analysis," Phys. Rev. Lett. **94**, 107204 (2005).

[23] F. Bloch, "Zur Theorie des Ferromagnetismus," Zeitschrift für Phys. **61**, 206–219 (1930).

[24] C. M. Srivastava and R. Aiyar, "Spin wave stiffness constants in some ferrimagnetics," J. Phys. C Solid State Phys. **20**, 1119–1128 (1987).

[25] J. Oitmaa and Weihong Zheng, "Curie and Néel temperatures of quantum magnets," J. Phys. Condens. Matter **16**, 8653–8660 (2004), arXiv:0409041 [arXiv:cond-mat].

[26] D Rodic, M Mitric, R Tellgren, H Rundlof, and A Kremenovic, "True magnetic structure of the ferrimagnetic garnet $Y_3Fe_5O_{12}$ and magnetic moments of iron ions," J. Magn. Magn. Mater. **191**, 137–145 (1999).

[27] Elmer E. Anderson, "Molecular field model and the magnetization of YIG," Phys. Rev. **134**, A1581 (1964).

Semi-quantum thermodynamics of complex ferrimagnets – Supplementary Information

Joseph Barker[1] and Gerrit E.W. Bauer[2,3]

[1]*Institute for Materials Research, Tohoku University, Sendai 980-8577, Japan*

[2]*Institute for Materials Research & AIMR & CSRN, Tohoku University, Sendai 980-8577, Japan*

[3]*Zernike Institute for Advanced Materials, University of Groningen, 9747 AG Groningen, The Netherlands*

S1 - QUANTUM THERMOSTAT

The quantum thermostat is difficult to implement in the time domain because the quantum fluctuation dissipation theorem is formulated as a function of frequency. One solution to this is to generate the stochastic noise making use of Fourier transforms [1]. A more memory-efficient method is to approximate the spectrum using stochastic differential equations. This approach was pioneered by Savin et al. for molecular dynamics [2]. The quantum fluctuation dissipation theorem for semi-quantum magnons does not include the zero-point energy (Eqs. 17-19 in Ref. [3]), we therefore omit these terms given from the expressions given by Ref. [2]. We reproduce the relevant equations in this supplementary material for completeness.

The effective field on each spin is given by (see main text)

$$\mathbf{H}_i(t) = \boldsymbol{\xi}_i(t) - \frac{1}{\mu_{s,i}} \frac{\partial \mathscr{H}}{\partial \mathbf{S}_i} \tag{S1}$$

where $\boldsymbol{\xi}_i(t)$ is the stochastic field of the thermostat. We work with coloured noise, but this has no memory of the spin dynamics, i.e. we disregard terms like $\mathbf{H}_i(t) = -\eta \int_{-\infty}^{t} \phi(t-t')(\partial \mathbf{S}_i/\partial t')dt'$.

The thermal noise on each lattice site, i, can then be written

$$\xi_{\alpha i}(t) = k_{\mathrm{B}}T \left(\frac{2\eta\mu_s}{\gamma\hbar} \right)^{1/2} \Phi_{i\alpha}(t) \tag{S2}$$

where $\alpha \in [x, y, z]$ is a Cartesian component, η is the coupling constant/damping parameter and $\Phi_{i\alpha}(t)$ is a stochastic processes obeying the quantum fluctuation-dissipation theorem. In this implementation it is approximated by the sum of two ancillary stochastic processes

$$\Phi_{i\alpha}(\tau) = c_0 \zeta_{0\alpha i}(\tau) + c_1 \zeta_{1\alpha i}(\tau) \tag{S3}$$

where $\tau = tk_{\mathrm{B}}T/\hbar$ is the reduced time, $c_0 = 1.8315, c_1 = 0.3429$. $\zeta_{i\alpha n}(\tau)$ is the solution of the second-order stochastic differential equations

$$\zeta''_{n\alpha i}(\tau) = \epsilon_{n\alpha i}(\tau) - \Omega_n^2 \zeta_{n\alpha i}(\tau) - \Gamma_n \zeta'_{n\alpha i}(\tau) \tag{S4}$$

where $\Omega_0 = 2.7189$, $\Omega_1 = 1.2223$, $\Gamma_0 = 5.0142$, $\Gamma_1 = 3.2974$, are constants to give a good approximation to the required noise spectrum (see Savin et al. [2]) and $\epsilon_{n\alpha i}(\tau)$ are white noise sources with the correlations:

$$\langle \epsilon_{n\alpha i}(\tau) \rangle = 0; \quad \langle \epsilon_{n\alpha i}(\tau) \epsilon_{k\beta j}(\tau') \rangle = 2\Gamma_n \delta_{\alpha\beta} \delta_{nk} \delta_{ij} \delta(\tau - \tau'). \tag{S5}$$

The stochastic process $\epsilon_{n\alpha i}(\tau)$ is generated using a pseudo random number generator with a normal distribution with mean 0 and width $(2\Gamma_n/\Delta\tau)^{1/2}$. $\zeta''_{i\alpha n}(\tau)$ is integrated with a fourth-order Runge-Kutta method with $\Delta t_\zeta = \Delta t_{\rm LLG} = 0.1$ fs. For the initial state we use $\zeta_{n\alpha i}(0) = \zeta'_{n\alpha i}(0) = 0$ and 'warm-up' the thermostat by integrating for 1 ns which colors the noise. After the warming up we, we start recording the spin dynamics of all sites.

S2 - VALIDATION FOR A GENERIC BCC FERROMAGNET

We performed a series of tests to validate the correct working of the method and the implementation. Using a generic BCC ferromagnetic model we compute thermodynamic properties and compare with available theoretical results. The nearest neighbour exchange energy is $J_{ij} = 3.5 \times 10^{-21}$ Joules, $\mu_s = 3\mu_{\rm B}$ unless stated otherwise, $\eta = 0.1$ and $\gamma = 1.76 \times 10^{-11}$ rad·s^{-1}·T^{-1}.

First, we compare simulated results with Bloch's law for the non-interacting magnon gas, which is valid at low temperatures (at which magnon-magnon interactions are negligibly weak). We test both the temperature dependence and also the $\mu_s = g\mu_{\rm B}\mathcal{S}$ dependence, which is absent in a fully classical formalism.

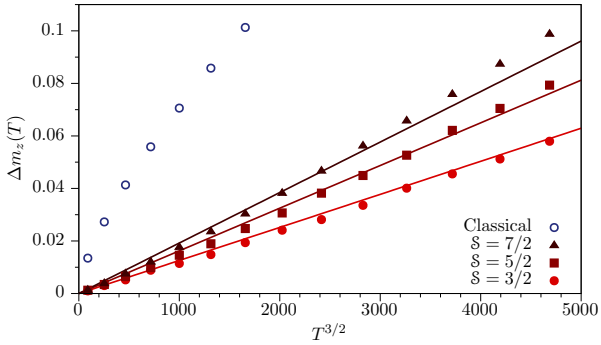

FIG. S1. Change in magnetization $\Delta m_z(T) = m_z(0) - m_z(T)$ as a function of temperature. Points are simulations and the lines are Bloch's law with no fitted parameters.

A similar Bloch's law analysis of the heat capacity, tests both temperature and $\mathcal{S}$ dependence. At the lowest temperature, $T = 1K$ we observe some deviation from the analytic behaviour because at such small amplitudes the errors in the integration become of the same order as the fluctuations $(\langle U_m^2\rangle_T - \langle U_m\rangle_T^2)$ of the internal energy.

With a quantum heat bath the Curie temperature T_C depends on the size of the magnetic moments (Fig. S3). This is the case also in 'fully quantum' Heisenberg models, but not in 'fully

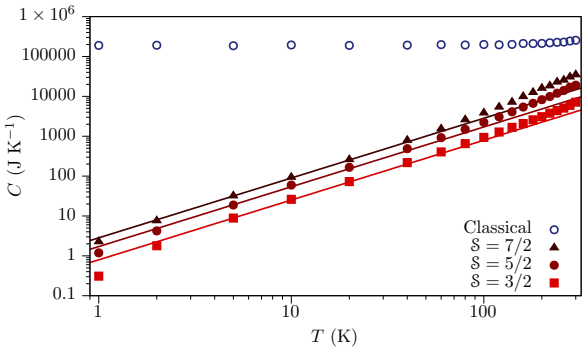

FIG. S2. Magnon heat capacity. Points are simulations and the lines are Bloch's law with no fitted parameters.

classical' Heisenberg models. We find good agreement with results for the quantum Heisenberg model and recover the classical result for large values of spin.

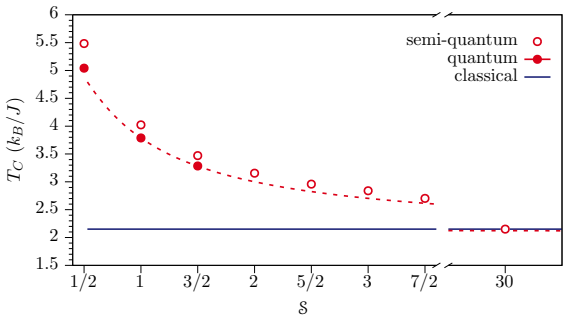

FIG. S3. Curie temperature as a function of $\mathcal{S}$. Classical result is from conventional spin dynamics calculation, quantum result is from Ref. [4]

As in quantum models the shape of the magnetisation curve now also depends on the size of the moment–for classical models it is independent of the moment (Fig. S4). It is well known both from experiments and theory that the shape of this curve depends on $\mathcal{S}$ [5]. The inability to reproduce this with classical statistics has been a major of previous models.

[1] Hichem Dammak, Yann Chalopin, Marine Laroche, Marc Hayoun, and Jean Jacques Greffet, "Quantum Thermal Bath for Molecular Dynamics Simulation," Physical Review Letters **103**, 190601 (2009).

[2] Alexander V. Savin, Yuriy A. Kosevich, and Andres Cantarero, "Semiquantum molecular dynamics

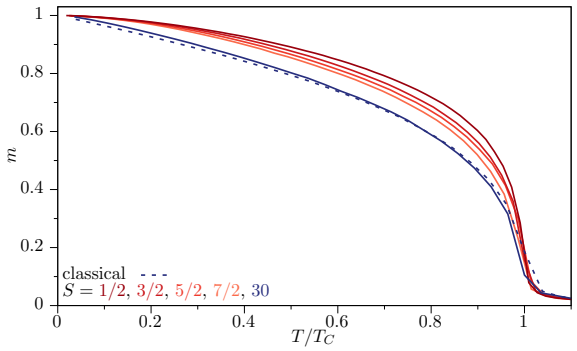

FIG. S4.

simulation of thermal properties and heat transport in low-dimensional nanostructures," Physical Review B **86**, 064305 (2012), arXiv:arXiv:1112.5919v2.

[3] C H Woo, Haohua Wen, A A Semenov, S L Dudarev, and Pui-wai Ma, "Quantum heat bath for spin-lattice dynamics," Physical Review B **91**, 104306 (2015).

[4] J. Oitmaa and Weihong Zheng, "Curie and Néel temperatures of quantum magnets," Journal of Physics Condensed Matter **16**, 8653–8660 (2004), arXiv:0409041 [arXiv:cond-mat].

[5] M.D. Kuz'min, "Shape of Temperature Dependence of Spontaneous Magnetization of Ferromagnets : Quantitative Analysis," Physical Review Letters **94**, 107204 (2005).